

Propagation of Rogue Waves and Cnoidal Waves Formations through Low Frequency Plasma Oscillations

Mrittika Ghosh¹, Sharry², Debiprosad Dutta³, S Chandra^{4*}

1Department of Physics, Midnapore College, West Bengal, India

2Department of Physics, Guru Nanak Dev University, Amritsar, Punjab.

3Behala College, Calcutta University, Kolkata, West Bengal.

4Government General Degree College, Kushmandi, West Bengal.

**Institute of Natural Sciences and Applied Technology, Kolkata, India, 700032.*

E-mail: ksharry799@gmail.com (corresponding author)

In this paper we consider the propagation of electron acoustic solitary waves in semi-classical plasma. Using quantum hydrodynamic model we obtain the dispersion relation and study the parametric variations of the dispersion curve. We further study the solitary profiles and its evolution by using the Korteweg-de Vries Burger equation. We extended our work to the study of Rogue waves. The results provide with interesting findings that has laboratory and astrophysical importance.

1. Introduction

A Star and hence our Sun, is almost entirely an ionized ball of plasma, consisting of electrons and ions, in which there is hardly any gas (or neutral atoms). In 1908 Kristian Birkeland observed the auroras and magnetic storms in nature and in his Terrella-experiment. He discussed his ideas on the solar wind, the origins of aurorae, and his terrella experiments in a lavish book, 'The Norwegian Aurora Polaris Expedition, 1902-1903 (1908-13)'. He immersed his terrella (small magnetized model ball representing the Earth) in plasma and found circular rings in the polar ends. These circular rings in the poles are now known as Auroras, Borealis and Australis. He made a set up in which he tried to explain magnetic storms. Birkeland never knew the structure of magnetosphere but current research follows Birkeland's lines. This created a connection between laboratory experiment and astrophysics.

The Gravitational fields are so weak that in case of astrophysics we can ignore general relativity. In case of various astrophysical objects relativistic effects play an important role or in some cases dominant role. Among these one is Neutron Star, a 'cold' star composed of neutrons majorly and is supported against collapse by neutron degeneracy pressure. Another is Super Massive Star, a giant object supported by radiation pressure, in which general relativity plays an important role in its stability and instability. And the most amazing of all these is Black Hole, a body caught in a gravitational collapse. In 1930's J. Robert Oppenheimer's work first put the ground theoretical work of Neutron Stars and Black Holes and 1960's the

joint effort of radio and optical astronomers revealed a great number of new objects.

Inside any star we get different types of pressures. The most common mode states the following pressures: inward pressure-gravitational pressure and outward pressure- pressure gradient. These two forces, i.e., gravitational force and the pressure gradient balance each other to stabilize a star. The origin of pressure gradient is the fuel of the star. Another pressure is radiation pressure. This pressure is formed inside the star. Photons randomly move and collide with the wall. This collision gives rise to radiation pressure. If gravitational pressure dominates over the pressure gradient and radiation pressure then the star starts collapsing. This can be stopped by electron degeneracy Pressure. According to Pauli's Exclusion Principal two electrons having same spin cannot stay in the same state. The plasma containing two groups of electrons occurs in both astrophysical environments [1, 2,3,4] as well as in laboratory experiments [5].

Another example is the Broadband Electrostatic Noise (BEN), which has been observed by the satellites missions [6, 7, and 8]. Two electron population plasmas usually follow Maxwellian distribution [9, 10], however some space and laboratory plasmas behave extremely different from Maxwellian distribution, where generalized Lorentzian or κ -distribution [11] comes into play. In recent years the study of EAWs became one of the prominent areas of research in physics of plasmas [12].

Most of the past studies are in the classical region. Such an example of semi classical plasma is the "corona" which is "high temperature-low density" plasma. However in some astrophysical

cases (e.g. neutron stars, white dwarfs etc) at very high densities the thermal pressure becomes negligible compared to Fermi pressure. In those situations Quantum and relativistic effects are taken into account. The purpose of the present paper is to investigate the linear and nonlinear properties of EAWs in semi classical plasma by deriving the linear dispersion relation and the KDV equation to study the formation of shock waves in EAW. The paper is arranged in the following manner: Section 2 contains the basic equations. Section 3 contains the derivation of linear dispersion relation. Section 4 contains the derivation Korteweg-de Vries Burgers equation using the standard perturbation techniques. Section 5 contains Rogue Waves and Section 6 contains Cnoidal Waves and finally we conclude the paper with practical observations.

2. Basic formulation

We consider the propagation of EAW in semi classical plasma consisting of two groups of electrons at different temperatures and stationary cold ions forming a uniform neutralizing background.

The dynamics of such plasma is governed by the following quantum hydrodynamic equations:

$$\frac{\partial(n_h)}{\partial t} + \frac{\partial(n_h u_h)}{\partial x} = 0 \quad (1)$$

$$\frac{\partial(n_c)}{\partial t} + \frac{\partial(n_c u_c)}{\partial x} = 0 \quad (2)$$

$$0 = \frac{1}{m_e} \left(e \frac{\partial \phi}{\partial x} - \frac{1}{n_h} \frac{\partial P_h}{\partial x} + \frac{\hbar^2}{2m_e} \frac{\partial}{\partial x} \left(\frac{1}{\sqrt{n_h}} \frac{\partial^2(\sqrt{n_h})}{\partial x^2} \right) \right) \quad (3)$$

$$\begin{aligned} & \left(\frac{\partial}{\partial t} + u_c \frac{\partial}{\partial x} \right) u_c = \\ & \left(e \frac{\partial \phi}{\partial x} + \frac{\hbar^2}{2m_e} \frac{\partial}{\partial x} \left(\frac{1}{\sqrt{n_c}} \frac{\partial^2(\sqrt{n_c})}{\partial x^2} \right) + n_c \frac{\partial^2 u_c}{\partial x^2} \right) \end{aligned} \quad (4)$$

$$\frac{\partial^2 \phi}{\partial x^2} = (n_c + n_h + z_i n_i) \quad (5)$$

Pressure Law

For Semi-Classical Case-

$$P_j = n_j k_B T_j \quad (6)$$

For Quantum Scale-

$$p_j = \frac{m_j v_{Fj}^2}{3n_{j0}^2} n_j^3 \quad (7)$$

Where the subscript j is used to denote hot electron (e_h) and cold electron (e_c), K_B is Boltzmann's constant, T_{Fe} is Fermi temperature.

Stretching

$$\xi = \epsilon^{\frac{1}{2}} (x - v_0 t) \text{ and } \tau = \epsilon^{\frac{3}{2}} t \quad (8)$$

Perturbation Expansion

$$\begin{bmatrix} n_j \\ u_j \\ \phi \end{bmatrix} = \begin{bmatrix} 1 \\ u_0 \\ \phi_0 \end{bmatrix} + \epsilon \begin{bmatrix} n_j^{(1)} \\ u_j^{(1)} \\ \phi^{(1)} \end{bmatrix} + \epsilon^2 \begin{bmatrix} n_j^{(2)} \\ u_j^{(2)} \\ \phi^{(2)} \end{bmatrix} + \dots \quad (9)$$

u_j And p_j are respectively the fluid velocity and pressure of the j^{th} species, \hbar is the Planck's constant divided by 2π ; ϕ is the electrostatic wave potential and Z_i is the charge of an ion.

Now using normalizing conditions

$$\bar{x} \Rightarrow \frac{x \omega_i}{v_{Fe}}, \quad \bar{t} \Rightarrow t \omega_i, \quad \bar{\phi} \Rightarrow \frac{e \phi}{2K_B T_{Fe}}, \quad \bar{n}_j \Rightarrow \frac{n_j}{n_0},$$

$$\bar{u}_j \Rightarrow \frac{u_j}{v_{Fe}}$$

$$\omega_e = \sqrt{\frac{4\pi n_0 e^2}{m_e}} \text{ is the Plasma Frequency } v_{Fe} = \sqrt{\frac{2K_B T_{Fe}}{m_e}} \text{ is the Fermi Velocity.}$$

The normalization wave equations become –

For Semi-Classical Case-

$$\frac{\partial(\bar{n}_h)}{\partial \bar{t}} + \frac{\partial(\bar{n}_h \bar{u}_h)}{\partial \bar{x}} = 0 \quad (10)$$

$$\frac{\partial(\bar{n}_c)}{\partial \bar{t}} + \frac{\partial(\bar{n}_c \bar{u}_c)}{\partial \bar{x}} = 0 \quad (11)$$

$$0 = \frac{\partial \bar{\phi}}{\partial \bar{x}} - \frac{1}{2\bar{n}_h} \frac{\partial \bar{n}_h}{\partial \bar{x}} + \frac{H^2}{2} \frac{\partial}{\partial \bar{x}} \left(\frac{1}{\sqrt{\bar{n}_h}} \frac{\partial^2 \sqrt{\bar{n}_h}}{\partial \bar{x}^2} \right) \quad (12)$$

$$\begin{aligned} & \left(\frac{\partial}{\partial \bar{t}} + \bar{u}_c \frac{\partial}{\partial \bar{x}} \right) \bar{u}_c = \\ & \left(\frac{\partial \bar{\phi}}{\partial \bar{x}} + \frac{H^2}{2} \frac{\partial}{\partial \bar{x}} \left(\frac{1}{\sqrt{\bar{n}_c}} \frac{\partial^2 \sqrt{\bar{n}_c}}{\partial \bar{x}^2} \right) + \eta_c \frac{\partial^2 \bar{u}_c}{\partial \bar{x}^2} \right) \end{aligned} \quad (13)$$

$$\frac{\partial^2 \bar{\phi}}{\partial \bar{x}^2} = (\bar{n}_c + \frac{\bar{n}_h}{\delta} - \bar{n}_i \frac{\delta_1}{\delta}) \quad (14)$$

For Quantum Scale-

$$\frac{\partial(\bar{n}_h)}{\partial \bar{t}} + \frac{\partial(\bar{n}_h \bar{u}_h)}{\partial \bar{x}} = 0 \quad (15)$$

$$\frac{\partial(\bar{n}_c)}{\partial \bar{t}} + \frac{\partial(\bar{n}_c \bar{u}_c)}{\partial \bar{x}} = 0 \quad (16)$$

$$0 = \frac{\partial \bar{\phi}}{\partial \bar{x}} - n_h \frac{\partial \bar{n}_h}{\partial \bar{x}} + \frac{H^2}{2} \frac{\partial}{\partial \bar{x}} \left(\frac{1}{\sqrt{\bar{n}_h}} \frac{\partial^2 \sqrt{\bar{n}_h}}{\partial \bar{x}^2} \right) \quad (17)$$

$$\begin{aligned} & \left(\frac{\partial}{\partial \bar{t}} + \bar{u}_c \frac{\partial}{\partial \bar{x}} \right) \bar{u}_c = \left(\frac{\partial \bar{\phi}}{\partial \bar{x}} + \right. \\ & \left. \frac{H^2}{2} \frac{\partial}{\partial \bar{x}} \left(\frac{1}{\sqrt{\bar{n}_c}} \frac{\partial^2 \sqrt{\bar{n}_c}}{\partial \bar{x}^2} \right) + \eta_c \frac{\partial^2 \bar{u}_c}{\partial \bar{x}^2} \right) \end{aligned} \quad (18)$$

$$\frac{\partial^2 \bar{\phi}}{\partial \bar{x}^2} = (\bar{n}_c + \frac{\bar{n}_h}{\delta} - \bar{n}_i \frac{\delta_1}{\delta}) \quad (19)$$

Here $H = \frac{\hbar \omega_c}{2K_B T_{Fe}}$ is a non dimensional quantum

parameter proportional to the quantum diffraction. The parameter H is proportional to the ratio

between the plasma energy $\hbar\omega$ (energy of an elementary excitation associated with an electron plasma wave) and $\delta = \frac{n_{eco}}{n_{eho}}$, $\delta_1 = \frac{z_i n_{i0}}{n_{eho}}$ Quasineutrality criteria reads $(1+\delta) = \delta_1$ the Fermi energy $k_B T_{Feh}$.

3. Dispersion characteristics

In order to study the linear dispersion characteristics of EAW in the plasma under consideration we assume that the field quantities vary as $e^{i(kx - \omega t)}$. To consider progressive and damping wave solution let us split the wavenumber (k) into real and imaginary segments (k_1 and k_2) respectively. Accordingly the frequency (ω) will also have real and imaginary segments (ω_{real} and $\omega_{imaginary}$). After some algebraic treatment we get the frequency of the progressive wave given by the dispersion relation [Eqns 20 and 21].

a) Dispersion characteristics for semi-classical plasma.

Now we assume the entire field variables are varying as $\exp [i(kx - \omega t)]$, we get normalized wave frequency $\omega = \omega_{real} + i \omega_{imaginary}$ and wave number $k = k_1 + ik_2$. we get following dispersion relation

$$\omega_{real} = u_0 k_1 + \eta_c k_1 k_2 + \frac{\delta(k_1^2 - k_2^2) \left(\frac{1}{2} + \frac{H^2}{4} (k_1^2 - k_2^2) \right) + (H^2 - \eta_c^2) \{ (k_1^2 - k_2^2)^2 - 4k_1^2 k_2^2 \}}{\sqrt{1 + (k_1^2 - k_2^2) \delta \left(\frac{1}{2} + \frac{H^2}{4} (k_1^2 - k_2^2) \right) + \frac{(H^2 - \eta_c^2) \{ (k_1^2 - k_2^2)^2 - 4k_1^2 k_2^2 \}}{4}}}$$

(20)

$$\omega_{imaginary} = u_0 k_2 - \frac{\frac{\eta_c}{2} (k_1^2 - k_2^2) + \frac{\delta(1+H^2 k_1 k_2)}{1+\delta(1+(H^2 k_1 k_2))} + (H^2 - \eta_c^2) k_1^2 k_2^2 (k_1^2 - k_2^2)}{\sqrt{1 + (k_1^2 - k_2^2) \delta \left(\frac{1}{2} + \frac{H^2}{4} (k_1^2 - k_2^2) \right) + \frac{(H^2 - \eta_c^2) \{ (k_1^2 - k_2^2)^2 - 4k_1^2 k_2^2 \}}{4}}}$$

Now, Figures (1,2,3) represents the long wave dispersion character in EAW's in semi classical plasma composed of hot electron and inertial cold electrons and stationary ions. We numerically examine the behavior of dispersion relation (20, 21) with respect to the variation of H, u_0 and η . Figure (1,2,3) shows the variation ω with k for different values of H, u_0, η . Figure (1), (2) and (3) shows ω - k curves for different values of H, u_0, η respectively. Obviously wave frequency ω also

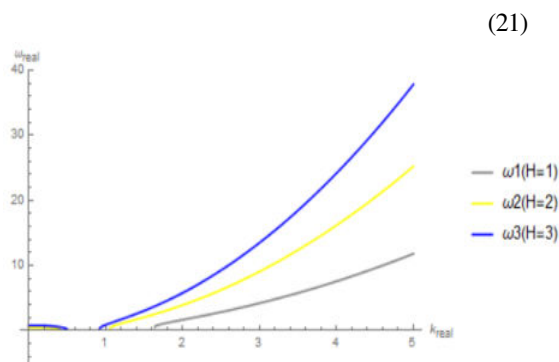


Fig. 1. Dispersion curves for different values of Quantum Diffraction Parameter (H) at constant $\delta = 0.6$ and $u_0 = 0.5$

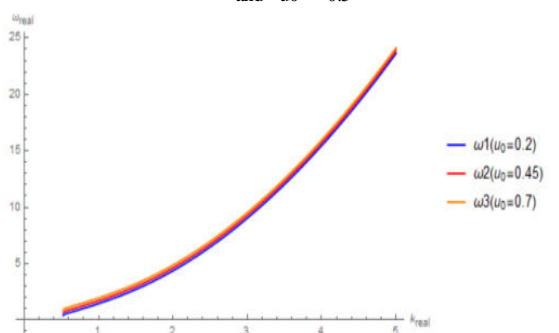


Fig. 2. Dispersion curves for different values of fluid velocity at constant $\delta = 0.6$ and $H=1$

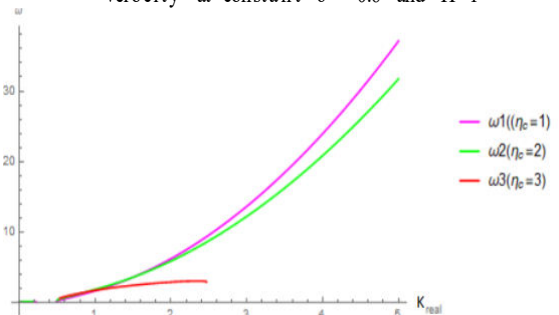


Fig.3. Dispersion curves for different values of charge neutrality at equilibrium ' δ ' at constant $u_0=0.5$ and $H=1$

increase with increase of the parameters. From Figure (1) we see that for the variation in H the relation between ω_{real} and k_1 get affected. The relation is non linear for very small value of k_1 nearly to 1.7. After that ω_{real} and k_1 behave classically (linearly). There is a certain bump or peak achieved at a certain point ($k_1=1.5$) in the non linear region. We also notice that the non linearity varies with variation of H in the non linear region. Whereas in the linear region there is no variation in

the figures. From Figure (2) we notice that the relation of ω_{real} and k_1 doesn't get effected due to variation in u_0 , and nearly linear for higher values of k_1 ($k_1 > 2$). From Figure (3) we notice that the graph between ω_{real} and k_1 has two region due to variation in η - Linear and Nonlinear Region, which also gets affected for different values of η .

$\eta=1$ and $\eta=2$ ($\eta < H$): The non-linearity is very slight and the nonlinear region is very short range for this case. The whole plot is nearly linear throughout the progression of k_1 . However slight change in slope occurs at $k_1 = 0.8$. $\eta=H=3$: Here no non linearity in observed due to the fact that the term in the R.H.S in equation (20) containing $(H^2 - \eta^2)$, becomes 0. So we can conclude that the non linearity comes only due to η . $\eta > 3$: Here the plot looks identical to Figure (1) where a nonlinear region is observed for $k_1 < 1$. Beyond which the plot becomes linear. A bump is also observed for $k_1=0.9$ in the non linear region.

Group velocity: The Group Velocity (c_g) of a wave is the velocity with which the overall envelop shape of the wave's amplitudes-known as the Modulation or Envelop of the wave-propagates through space.

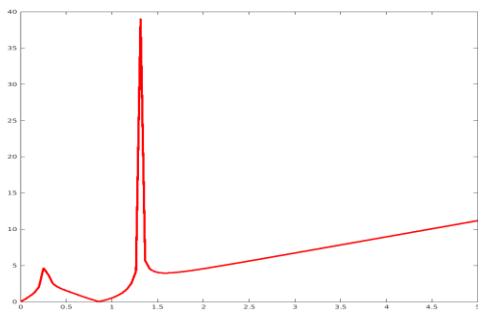


Fig. 4 Group velocity (c_g) vs wavenumber (k)

$c_g = \frac{d\omega}{dk}$ Vs k graph is drawn with the variation of H in Figure (4). The Figure has two regions Linear ($k_1 > 1.5$) and Non linear ($k_1 < 1.5$). We observe two peaks in the non linear region at nearly 0.25 and 1.4 respectively.

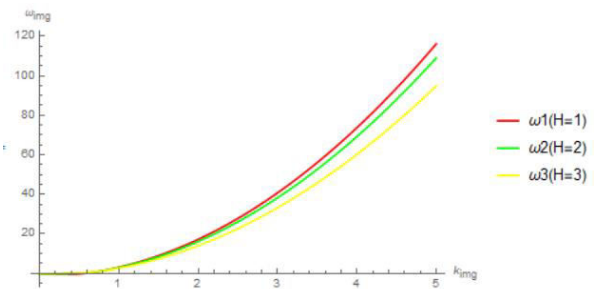


Fig. 5. $\omega_{imaginary}$ vs k_2 Variation of H

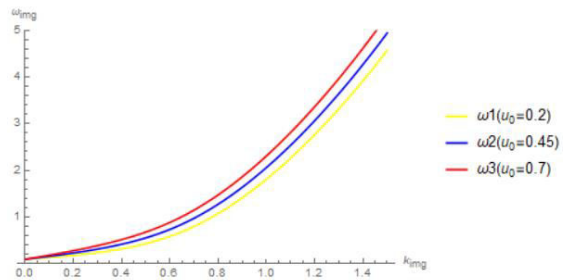


Fig. 6. $\omega_{imaginary}$ vs k_2 Variation of u_0

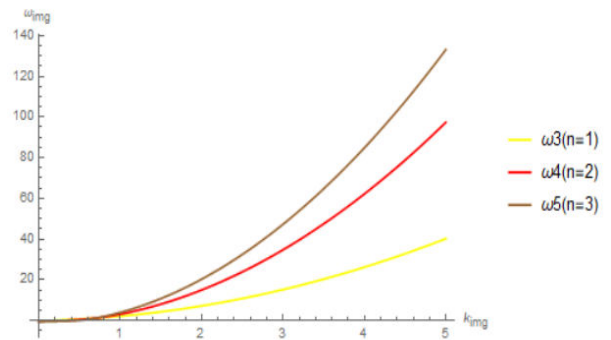


Fig. 7. $\omega_{imaginary}$ vs k_2 Variation of η

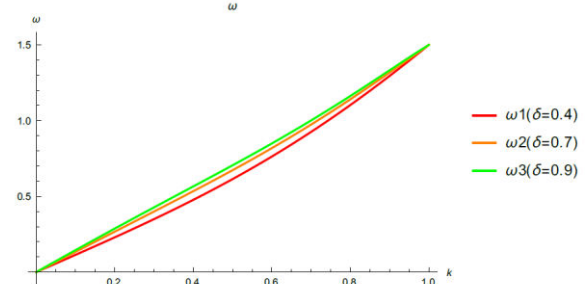


Fig.8. Dispersion curves for different values of charge neutrality at equilibrium δ at constant $u_0=0.5$ and $H=2$

From Figure (5) we see that the relation between $\omega_{imaginary}$ and k_2 is linear for $k_2 > 1$. For $H=1$ and $H=2$ the variation is very low and non linearity is very slight and the two plot intersect (ie possesses same value of $\omega_{imaginary}$) for $k_2=0.8$ For $H=3$ the graph is non linear till $k_2=0.9$ and a bump is

observed in $k_2=0.8$. From Figure (6) we see that the relation of $\omega_{imaginary}$ and k_2 doesn't get affected due to the variation of u_0 and nearly linear for values greater than $k_2>1$. From Figure (7) we see that the graph between $\omega_{imaginary}$ and k_2 has two region due to variation in η - Linear and Non linear Region, which also gets affected for different values of η . $\eta>H(=3)$: The non linearity is very slight and the non linear region is very short range for this case. The whole plot is nearly linear throughout the progression of k_2 . However slight change in slope occurs at $k_2 = 0.6$.

$\eta=H=3$: Here no non linearity is observed due to the fact that the term in the R.H.S in equation (21) containing $(H^2 - \eta^2)$, becomes 0. So we can conclude that the non linearity comes only due to η . $\eta<H$: Here the plot looks identical to Figure (5) where a non linear region is observed for $k_2<1$. Beyond which the plot becomes linear. A bump is also observed for k_2 between 0.8 and 0.9 in the nonlinear region. All the graphs intersect on a single point and the gives the same value of $\omega_{imaginary}$ at $k_2 = 0.7$.

b) Dispersion characteristics for Fermi plasma

Assuming that all the field quantities vary as $\exp[i(kx - \omega t)]$, then for normalized wave frequency and wave number k , we get Dispersion Relation

$$1 = \frac{1}{(\omega - ku_0)^2 - \frac{H^2 k^4}{4}} - \frac{\frac{1}{\delta}}{k^2 - \frac{H^2 k^4}{4}} \quad (22)$$

We numerically examine the behavior of dispersion relation with respect to variations of, H and u_0 . In all the three cases i.e. Fig.(8), Fig.(9) and Fig.(10), there is an increase in the slope of dispersion curve i.e. the phase velocity $(\frac{\omega}{k})$ increases with increase in value of either any one or all three of the parameters. In Fig.(8), as we shift to higher values of δ the $\omega - k$ graph also shifts to higher value, however the variation is not much. As δ is the ratio of number density of electrons to that of holes, it implies more will be the number density of Electrons as compared to holes, higher will be the curve. Also we can see, the variation of ω with k occurs more rapidly at higher value of Fig. 8. Dispersion curves for different values of charge neutrality at equilibrium ' δ ' at constant $u_0 = 0.5$ and $H=2$ charge neutrality at equilibrium (δ) but becomes the same at higher value of k . In Fig.(9),the slope of dispersion curve increases with

increase in value of H . Quantum Diffraction Parameter is ratio of plasma energy to Fermi energy of paired particles. Growing H broadens the range of permitted frequencies but after a certain point. Before that point, the curves are identical In Fig.(10),In this case, again, the phase velocity $(\frac{\omega}{k})$ increases weakly with increase in the value of u_0 .

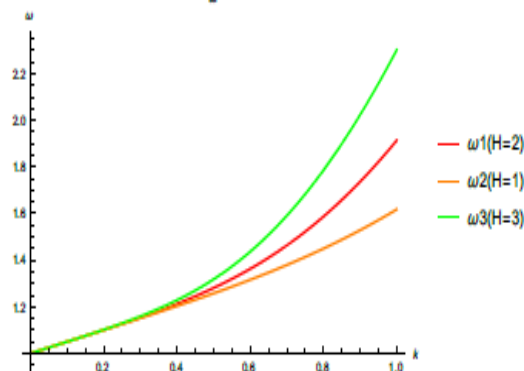


Fig. 9. Dispersion curves for different values of Quantum Diffraction Parameter (H) at constant $\delta = 0.6$ and $u_0 = 0.5$

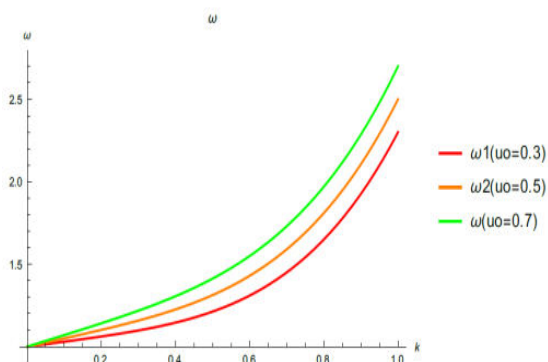


Fig. 10 Dispersion curves for different values of fluid velocity at constant $\delta = 0.6$ and $H=2$

4. Derivation of KdV-Burgers Equation

In order to derive the equation of motion for nonlinear electron acoustic wave, we use the reductive perturbation method and the stretched coordinates as defined before.

After doing some algebraic operations, we will obtain following KDV-B equation

$$\left(\frac{\partial}{\partial \tau} \phi^{(1)} + A \phi^{(1)} \frac{\partial}{\partial \xi} \phi^{(1)} + B \frac{\partial^3}{\partial \xi^3} \phi^{(1)} - C \frac{\partial^2}{\partial \xi^2} \phi^{(1)} \right) = 0 \quad (22)$$

For Semi-Classical Plasma-

$$A = \frac{4R^4 - 3}{2R}, B = \frac{4R^4 - H^2(1+R^4)}{2R}, C = \left(-\frac{\eta_0}{2} \right)$$

And For Fermi Plasma-

$$A = - \left[\frac{2(V_0 - u_0)^2 + 1}{(V_0 - u_0)[(u_0 - V_0)^2 + 1]} \right]$$

$$B = - \frac{H^2}{4(V_0 - u_0)[(u_0 - V_0)^2 + 1]} \text{ and } C = \frac{\eta_{co}}{[(u_0 - V_0)^2 + 1]}$$

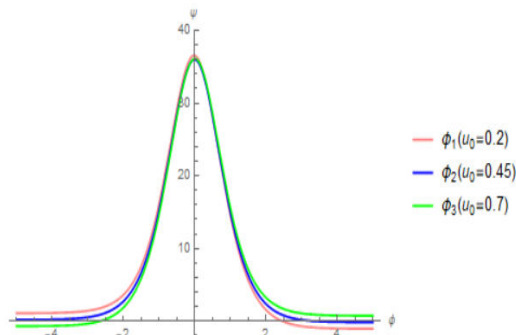


Fig. 11. ψ vs. ξ Variation of u_0

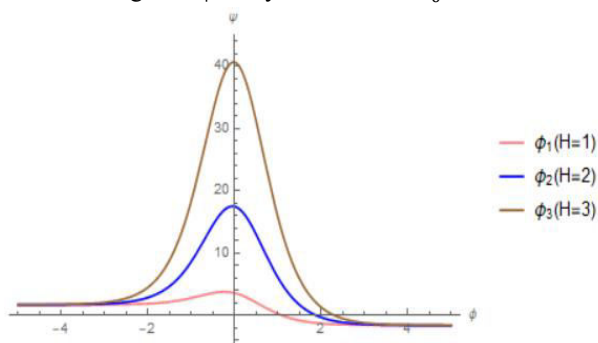


Fig. 12. ψ vs ξ Variation of H

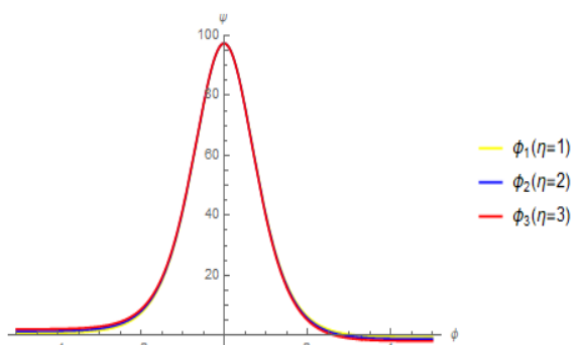


Fig. 13. ψ vs ξ Variation of η

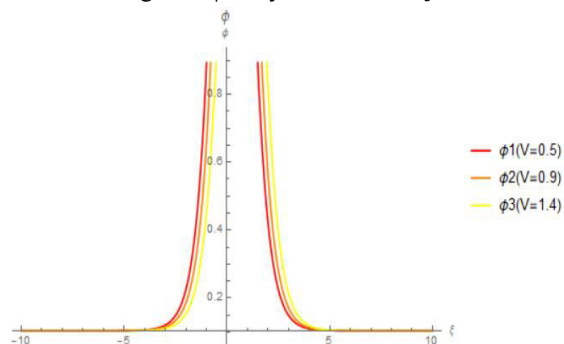


Fig. 14. ϕ is plotted for different values of Quantum Diffraction Parameter (H) for $m=0.2$ and $\eta=0.2$

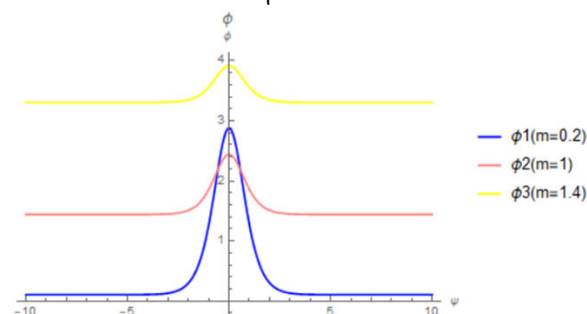


Fig. 15. ϕ is plotted for different values of $V_0 - u_0(m)$ for $H=1$ and $\eta=0.2$

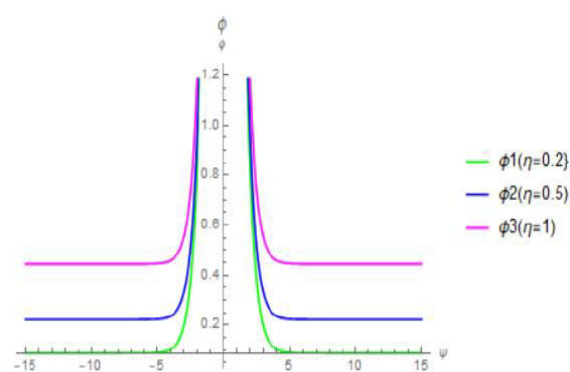


Fig. 16. ϕ is plotted for different values of Viscosity coefficient (η) for $H=2$ and $m=0.2$

In order to solve the Kdv Burgers equation we introduce a transformation

$$\psi = \xi - Mt \tag{23}$$

where M is the Mach Number (ie. Speed of the frame), η is the new phase variable combining both ' ξ ' and ' τ ' into a single variable.

We can study the evolution of the Shock Profiles of Kdv Burgers equations. The boundary conditions are given as $\xi \rightarrow 0$ we get $\psi \rightarrow 0$ $\frac{\partial^2 \psi}{\partial \xi^2} \rightarrow 0 \rightarrow 0$.

The solution of Kdv Burgers equations

$$\phi = \frac{12B}{A} \text{sech}^2 \psi - \frac{36C}{15A} \tanh \psi \tag{24}$$

The above equation comprises of Solitary Structure (1st part) and Shock component 2nd part).

5. Rogue waves

Rogue Waves are surface waves. They are much higher than the other waves and are usually created in Open Ocean. Unlike normal ocean waves which

allow the ship to rise and fall relatively gently, these waves have very short wavelength and as a result it is extensively stiff. Tsunami must not be confused with Rogue Waves. Tsunami consists of series of waves that move through the entire water column usually caused due to an undersea earth quake. In the open ocean due to the long wavelength of multiple hundred kilometers one will even not notice when these waves pass below their ship. Fig. 16. φ is plotted for different values of Viscosity coefficient (η) for $H=2$ and $m=0.2$ These waves when hit the coast, slow down and get compressed and they grow to large heights. Rogue waves on the other hand arise from typical ocean waves and only effect relatively small quantities of surface water. They can build up from very calm and apparently safe Sea Water and thus is very dangerous. They arise in the open ocean and last for a short time, disappearing the way they form. In shallow waters, they would quickly become unstable and collapse creating no real problem to coast. But in the sea, they are devastating and can destroy even modern-day ships. Numerous ships are lost due to rogue waves. Rogue Waves are of different types-

- Single wave- Giant storm waves which build up to enormous heights and usually collapse after a few seconds.
- Walls of water- A wide wave walls that last much longer and travel a large distance in oceans

- Three sisters- close successive waves. The properties of electron acoustic rogue waves in a three component plasma system consisting of electrons, cold electrons and stationary ions have been investigated.

The occurrence of rogue waves in plasma can be adjusted by varying the parameters. The results of this may be applicable in space plasma. To find an explanation for them we can take the help of Non Linear Schrodinger Equations. It can be shown that it is possible for different wave components to act and exchange energy. In rare but frequent cases these integration can produce instability that allows the waves to suck energy in all the other waves surrounding it growing into Rogue wave. A non linear wave in Plasma named accordingly Rogue waves can be explained by NLSE

The general Kdv-B equation states

$$A \frac{\partial \varphi}{\partial \tau} + A_1 \frac{\partial \varphi}{\partial \xi} + A_2 \varphi^2 \frac{\partial \varphi}{\partial \xi} + B \frac{\partial^3 \varphi}{\partial \xi^3} + R \frac{\partial^2 \varphi}{\partial \xi^2} = 0$$

Fourier expansion

$$\varphi = \epsilon^2 \varphi_0 + \epsilon \varphi_1 e^{i\psi} + \epsilon \varphi_1^* e^{-i\psi} + \epsilon^2 \varphi_2 e^{i2\psi} + \epsilon^2 \varphi_2^* e^{-i2\psi} + \dots$$

$$\psi = k\rho - \omega\theta$$

Perturbation equation

$$\varphi_0 = \varphi_0^{(1)} + \epsilon \varphi_0^{(2)} + \epsilon^2 \varphi_0^{(3)} \dots$$

$$\varphi_1 = \varphi_1^{(1)} + \epsilon \varphi_1^{(2)} + \epsilon^2 \varphi_1^{(3)} \dots$$

$$\varphi_2 = \varphi_2^{(1)} + \epsilon \varphi_2^{(2)} + \epsilon^2 \varphi_2^{(3)} \dots$$

Group velocity

$$c = \frac{d\omega}{dk} = \frac{3Bk^2}{A_0}$$

Again we have to use the stretched variables as,

$$\rho = \epsilon(\xi - c\tau) \text{ and } \theta = \epsilon^2 \tau$$

Therefore,

$$\frac{\partial}{\partial \tau} = -is\omega - \epsilon c \frac{\partial}{\partial \rho} + \epsilon^2 \frac{\partial}{\partial \theta}$$

$$\frac{\partial}{\partial \xi} = isk + \epsilon \frac{\partial}{\partial \rho}$$

Here, s is the order of the wave function.

The complex Nonlinear Schrodinger equation of First type:

$$i \left(\frac{\partial \varphi}{\partial \theta} \right) - P \left(\frac{\partial^2 \varphi}{\partial \rho^2} \right) = Q (\varphi^* \varphi) \varphi$$

Where,

$$P = \left(\frac{3Bk - iR}{A_0} \right)$$

$$Q = \left[\frac{A_1^2 k}{A_0} \left(\frac{1}{(6Bk^2 + i4kR)} - \frac{1}{3Bk^2} \right) \right]$$

Going to higher order of both harmonics and perturbation scale factors we obtain complex Nonlinear Schrodinger equation of Second type

$$i \left(\frac{\partial \varphi}{\partial \theta} \right) - P_1 \left[\left(\frac{\partial^2 \varphi}{\partial \rho^2} \right) + \frac{1}{\theta} \left(\frac{\partial \varphi}{\partial \rho} \right) \right] = Q_1 (\varphi^* \varphi) \varphi \quad (25)$$

$$P_1 = \left(\frac{6Bk - iR}{A_0} \right) \left(\frac{2A_1}{6Bk^2 + i4kR} \right)$$

$$Q_1 = \left[-\frac{2A_1^2 k}{3Bk^2} \left(\frac{A_1}{6Bk^2 + i4kR} \right) + 4kA_2 \right] \left(\frac{6Bk^2 + i4kR}{2A_1 A_0} \right)$$

Solving the NLSE

$$i\frac{\partial\varphi}{\partial\theta} + P\frac{\partial^2\varphi}{\partial\rho^2} = -Q\varphi\varphi\varphi^* \quad (26)$$

$$\varphi(\rho, \theta) = \sqrt{\frac{2P}{Q}} \left[\frac{4(1 + 4iP\theta)}{1 + 16P^2\theta^2 + 4\rho^2} - 1 \right] \exp(2iP\theta)$$

Note the $-Q$ on RHS, and $+P$ on LHS, change signs accordingly.

From the given Kdv-B equation we get the values of P and Q , $A_0 = 1$, $A_1 = A = \frac{4R^4 - 3}{2R}$, $A_2 = 0$, $B =$

$$B = \frac{4R^4 - H^2(1 + R^4)}{2R}, \quad R = -C = \frac{\eta - c}{2}$$

$$P = \left(\frac{3Bk - iR}{A_0} \right) = (3Bk - iR), \quad Q = \left[\frac{A_1^2 k}{A_0} \left(\frac{1}{(6Bk^2 + i4kR)} - \frac{1}{3Bk^2} \right) \right]$$

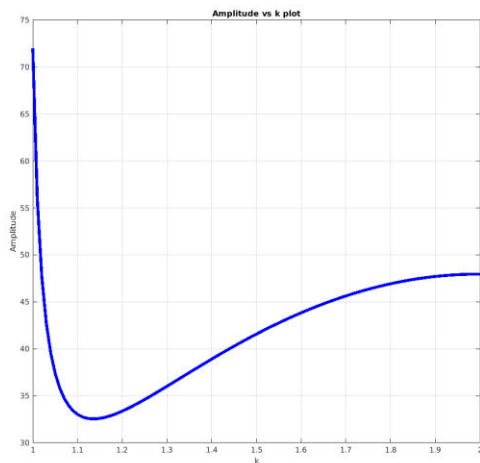


Fig17 Amplitude vs Wave number

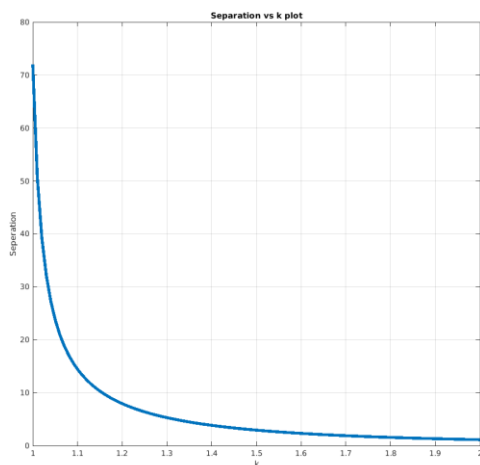


Fig.18 Separation of Wave number

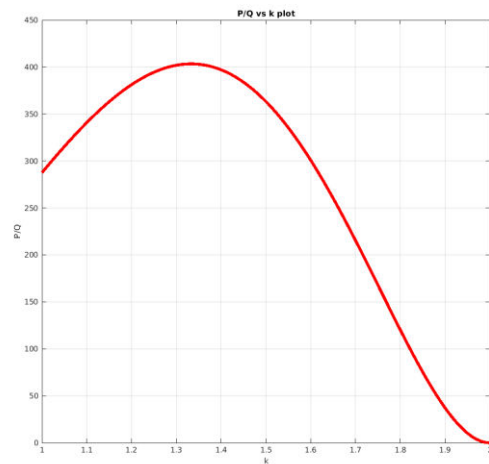


Fig 19 P/Q vs Wave number

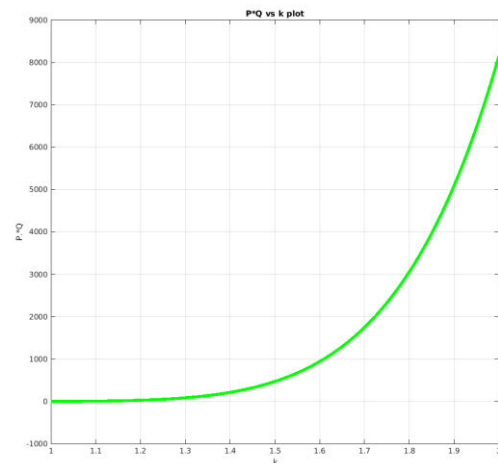


Fig. 20 P*Q vs Wave Number

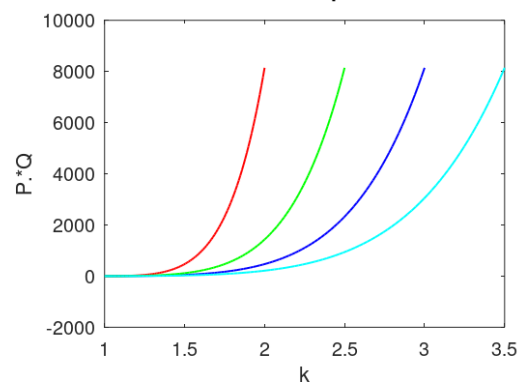


Fig 21 P*Q vs K with variation in H

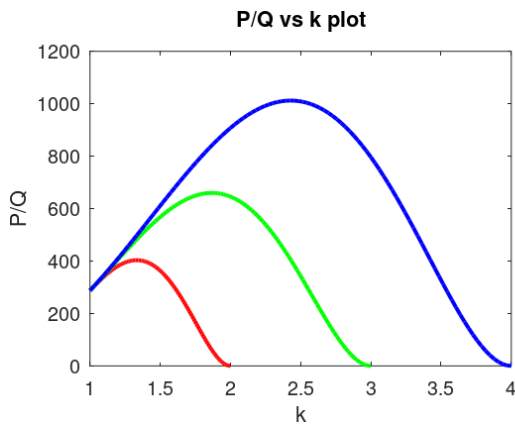


Fig 22 P/Q vs K with the variation of H

6. Cnoidal waves

In fluid dynamics, a cnoidal wave is a nonlinear and exact periodic wave solution of the Korteweg–de Vries equation and in the limit of infinity Wavelength turn into solitary waves. Unlike Rogue Waves, these waves characterize sharper crests and flatter troughs. These solutions are in terms of the Jacobi elliptic function cn , which is why they are Coined cnoidal waves. They are used to describe surface gravity waves of Fairly long wavelength, as compared to the water Depth. Nonlinear cnoidal waves such as dnoidal (dn) Are found in the defocusing region of ionospheric Plasma. To investigate the steady-state solution of Electron Acoustic Waves (EAW) cnoidal waves of KdVB equation, we use $\eta = \xi - v\tau$ transformation, where v is the velocity of cnoidal waves moving with the frame. Equation 24 transforms to

$$B \frac{\partial^2 \psi}{\partial \eta^2} + C \frac{d\psi}{d\eta} - V_1 \psi + A\psi^2 = 0 \quad (27)$$

$$\frac{1}{2} \left(\frac{d\psi}{d\eta} \right)^2 + V(\psi) = E(\psi) \quad (28)$$

Where,

$$V(\psi) = \frac{D}{3B} \psi^3 - \frac{V_1}{2B} \psi^2$$

And

$$E(\psi) = \frac{-C}{B} \int \frac{d\psi}{d\eta} d\psi$$

Where $E(\psi)$ is the Total Energy and becomes constant of motion for the case $C=0$. Note that the potential $V(\psi)$ is asymmetric and corresponds to the potential of Helmholtz Oscillator. In the figure we have solution of the Cnoidal Wave for $C=0$ case which is given below-

$$\psi(\eta) = \psi_1 + \psi_c \text{cn}^2(D\eta, m) \quad (29)$$

Where cn is the Jacobi elliptic function,

$$D = \sqrt{\frac{A(\psi_3 - \psi_1)}{6B}},$$

$$m = \frac{\sqrt{3} - \psi_2}{\psi_3 - \psi_1}$$

And

$$\psi_c = \psi_3 - \psi_2$$

The pseudopotential roots,

$$\psi_{12} = \frac{V_1}{2A} - \frac{(1 \pm i\sqrt{3})V^2}{4AT} - \frac{(1 \pm i\sqrt{3})}{4A} T$$

The energy depletion coefficient is

$$T = V^3 + 12B^2 A E_0 + 2\sqrt{6} \sqrt{BV^3 A^2 E_0 + 6B^2 A^4 E_0^2}$$

Now, for $m \rightarrow 1$ and $E_0 = 0$ the cnoidal wave solution approaches to solitary wave solution (where we do $\psi_1 = \psi_2 = 0$).

$$\psi_c = \psi_3 = \frac{1}{2} \left(\frac{V}{A} + \frac{1}{AV} + \frac{V^3}{A} \right) = \psi_m$$

$$D = \sqrt{\frac{A\psi_m}{6B}} = \frac{1}{N}$$

In the limiting case, the Jacobi elliptic function $Cn(x)$ degenerates to $\text{sech}(x)$ from equation of EAW solitary solution is

$$\psi(\eta) = \psi_m \text{sech}^2 \frac{\eta}{W} \quad (30)$$

Where ψ_m and W are the peak amplitude and width of the solitary wave respectively.

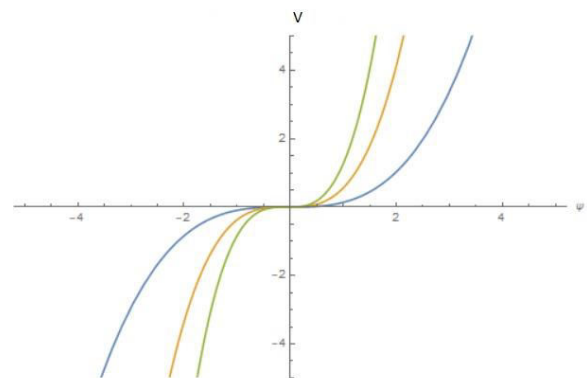


Fig. 23. $V(\psi)$ vs ψ

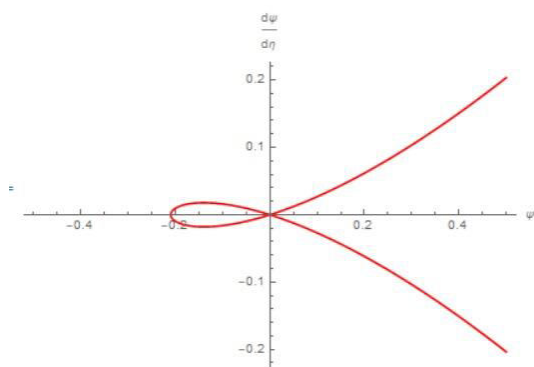


Fig. 24. (ψ') vs ψ

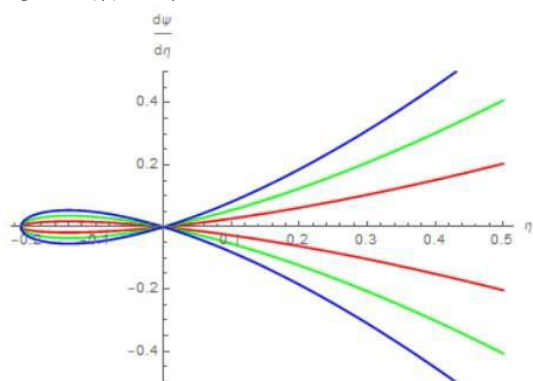


Fig 25. (ψ') vs ψ with the variation of H

7. Results and Discussions

In this paper we have done detailed study of space plasma driven by Classical as well as Quantum pressure laws. Stars are giant balls of plasma, where a burning/fusing core supplies the energy of the star to complete its stellar evolution. There are lots of Component forces acting inside a star, maintaining the stability of the star. One component of the pressure in a star is the gas pressure or particle pressure. As the large mass of hydrogen and helium gas and dust (the protostar) begins to contract as a result of its gravitational forces, increased particle speed and collisions cause the average particle kinetic energy to increase. From the idea of kinetic temperature, it follows that there is an increased temperature and an associated pressure. Starting the process of evaluating particle pressure with an ideal monoatomic gas, the Maxwell-Boltzmann velocity distribution can be used. The resulting expression for particle pressure is $P_{\text{particle}} = nkT$. Where n is the number density of particles, k is Boltzmann's constant and T the temperature. This can be used a first estimate of particle pressures in stars. The Classical pressure is applicable for young stars which have enough fuel to burn towards their Red-giant or Super-giant

phase. Betelgeuse, in constellation of Orion, is an example of a star in Red giant phase. But, when the triple-alpha process in a red giant star is complete, those evolving from stars less than 4 solar masses do not have enough energy to ignite the carbon fusion process. They collapse, moving down of the main sequence until their collapse is halted by the pressure arising from electron degeneracy where Pauli Exclusion Principle comes into play. Electron degeneracy is a stellar application of the Pauli Exclusion Principle, as is neutron degeneracy. No two electrons can occupy identical states, even under the pressure of a collapsing star of several solar masses. For stellar masses less than about 1.44 solar masses, the energy from the gravitational collapse is not sufficient to produce the neutrons of a neutron star, so the collapse is halted by electron degeneracy to form white dwarfs. An interesting example of a white dwarf is Sirius-B. Sirius-B gives an example of the size of a white dwarf. Electron degeneracy halts the collapse of this star at the white dwarf stage. We have worked with semi classical plasma containing hot electron, cold electron and ion creating a neutralizing atmosphere. We have derived the dispersion relation which contains both real and imaginary part. We have worked with two different pressure laws. The imaginary part proves the damping characteristics which destroys the principal of conservation of energy. Figure (1-3) shows w_{real} Vs k_{real} graph plotted with the variation of H, u_0 and η . Fig.(5-7) shows the variation of $w_{\text{imaginary}}$ and $k_{\text{imaginary}}$ for different values of streaming velocity u_0 . The real part characterizes the free propagation of the wave while the imaginary part results in damping. It was first Landau who observed the imaginary part of w . So the EAW will be a heavily damped as the wave velocity is comparable to electron velocity. Fig. (9-10) shows the same with fermi plasma. Hereafter, we examine the likelihood of the electron-acoustic rogue wave's propagation in Maxwellian as well as Quantum plasma in the framework of the Korteweg-de Vries (KdV) equation. For this purpose, we use the reductive perturbation technique to carry out this study. It is known that the families of the KdV equations have solutions of distinct structures such as solitons, shocks, kinks, cnoidal waves, etc. However, our prime focus was only on rogue waves and cnoidal waves. Again, the dynamics of the nonlinear rogue waves is governed by the nonlinear Schrödinger equation (NLSE).

Thus, the KdV equation is transformed to their corresponding NLSE developing a weakly nonlinear wave packet. We show the possible region for the existence of the rogue waves and define it precisely for typical parameters of space plasmas. Figure (11-13) shows the shock profile for different values of streaming velocity u_0 , quantum diffraction parameter H , and η . It shows that a slight change in H increases the amplitude. In figure (14-16) the variation of ξ shows the steeper characteristics of shock waves. It shows the solitonic like structures in plasmas which leads to nonlinear waves. To conclude, we have studied for the first time the ion-acoustic cnoidal waves and solitons in unmagnetized Quantum plasma. The KdV equation for ion-acoustic waves in quantum plasma was obtained using the reductive perturbation method with periodic wave boundary conditions, appropriate to study cnoidal waves. It is found that both Compressive and rarefactive nonlinear ion-acoustic cnoidal wave structures are formed in such degenerate plasma, which depends on the quantum parameter. The dependence of wave frequency and wavelengths on the non-Linear ion-acoustic wave amplitude is also investigated at different values of quantum parameters with the degenerate Plasma densities exist in astrophysical and laboratory plasmas. It is found that the dependencies of wavelength and frequency on wave amplitude at different quantum parameters. For electrons behave differently for compressive and rarefactive ion-acoustic cnoidal wave cases. The results are useful to understand how nonlinear wave propagates in quantum plasmas.

Acknowledgments

The authors would like to thank the reviewers for their valuable inputs towards upgrading the paper. Authors would also like to thank the Institute of Natural Sciences and Applied Technology, the Physics departments of Jadavpur University and Government General Degree College at Kushmandi for providing facilities to carry this work.

References

[1] M. F. Thomsen, S. P. Gary, W. C. Feldman, T. E. Cole, and H. C. Barr. Stability of electron distributions within the earth's bow shock.

Journal of Geophysical Research, 88:3035–3045, April 1983.

[2] W.C. Feldman, R.C. Anderson, S.J. Bame, S.P. Gary, J.T. Gosling, D. J. McComas, M.F. Thomsen, G. Paschmann, and M. M. Hoppe. Electron velocity distributions near the earth's bow shock. Journal of Geophysical Research, 88:96–110, January 1983.

[3] S. D. Bale, P. J. Kellogg, D. E. Larsen, R. P. Lin, K. Goetz, and R. P. Lepping. Bipolar electrostatic structures in the shock transition region: Evidence of electron phase space holes. Geophysical Research Letters, 25:2929–2932, 1998.

[4] C. S. Lin, J. L. Burch, S. D. Shawhan, and D. A. Gurnett. Correlation of auroral hiss and upward electron beams near the polar cusp. Journal of Geophysical Research, 89:925–935, February 1984.

[5] Defler and Simonen (1969), Henry and Trguier (1972), Kadomtsev and Pogutse (1971), Armstrong et al. (1979), Sheridan et al. (1991), Ditmire et al. (1998).

[6] H. Matsumoto, H. Kojima, T. Miyatake, Y. Omura, M. Okada, I. Nagano, and M. Tsutsui. Electrotastic Solitary Waves (ESW) in the magnetotail: BEN wave forms observed by GEOTAIL. Geophysical Research Letters, 21:2915–2918, December 1994.

[7] J. R. Franz, P. M. Kintner, and J. S. Pickett. POLAR observations of coherent electric field structures. Geophysical Research Letters, 25:1277–1280, 1998.

[8] C. A. Cattell, J. Dombeck, J. R. Wygant, M. K. Hudson, F. S. Mozer, M. A. Temerin, W. K. Peterson, C. A. Kletzing, C. T. Russell, and R. F. Pfaff. Comparisons of Polar satellite observations of solitary wave velocities in the plasma sheet boundary and the high altitude cusp to those in the auroral zone. Geophysical Research Letters, 26:425–428, 1999.

[9] K. Nishihara and M. Tajiri. Rarefaction ion acoustic solitons in two electron-temperature plasma. Journal of the Physical Society of Japan, 50:4047–4053, December 1981.

[10] M. P. Leubner. On Jupiter's whistler emission. Journal of Geophysical Research, 87:6335–6338, August 1982.

[11] T. K. Baluku and M. A. Hellberg. Dust acoustic solitons in plasmas with kappa-distributed electrons

and/or ions. *Physics of Plasmas*,15(12):123705, December 2008.

[12] Singh and Lakhina 2001, Sultana and Kourakis 2011, Kourakis and shukla 2004

[13] S. Chandra, S. N. Paul, and B. Ghosh, "Electron-acoustic solitary waves in a relativistically degenerate quantum plasma with two-temperature electrons", *Astrophysics and Space Science*, vol. 343, no. 1, pp. 213–219,2013.

[14] H. R. Pakzad and K. Javidan, "Ion acoustic shock waves in weaklyrelativistic and dissipative plasmas with nonthermal electrons and thermal positrons", *Astrophysics and Space Science*, vol. 331, no. 1, pp. 175–180,2011.

[15] Wazwaz, Abdul-Majid. "New travelling wave solutions to the Boussinesq and the Klein–Gordon equations." *Communications in Nonlinear Science and Numerical Simulation*", 13.5 (2008): 889-901.

[16] J. Goswami, S. Chandra, and B. Ghosh, "Shock waves and the formation of solitary structures in electron acoustic wave in inner magnetosphere plasma with relativistically degenerate particles", *Astrophysics and Space Science*, vol. 364, no. 4, p. 65, 2019.

Received: 21st October 2020

Accepted: 21st December 2020